Ab initio calculation of interstitial-atom effects in $YFe_{10}Mo_2X$ ($X=E$,H,B,C,N,O,F)

Jinbo Yang, Weihua Mao, and Yingchang Yang
Department of Physics, Peking University, Beijing 100871, People's Republic of China

Senlin Ge
Beijing University of Posts and Telecommunications, Beijing 100088, People's Republic of China

Dongfeng Chen
Institute of Atomic Energy, Academic Sinica, Beijing 102413, People's Republic of China
(Received 5 May 1997; revised manuscript received 13 August 1997)

Neutron diffraction was used to determine the crystallographic structures of the $YFe_{10}Mo_2$ and $YFe_{10}Mo_2X$ (X=H,N). The spin-polarized muffin-tin-orbital method was applied to calculate the electronic structures of $YFe_{10}Mo_2X$ (X=H,B,C,N,O,F) and $YFe_{10}Mo_2E$, which is $YFe_{10}Mo_2$ with an empty sphere insertion. Both N and H atoms were found to reside on the interstitial 2*b* sites. The magnetovolume effect and chemical bonding effect of interstitial X atoms are investigated by a systematic analysis of the local magnetic moments $\mu_{\rm loc}$, Fermi-contact hyperfine fields ($H_{\rm FC}$), and isomer shifts (IS) at different Fe sites in $YFe_{10}Mo_2X$ (X=H,B,C,N,O,F) and $YFe_{10}Mo_2E$. It is found that the insertion of the X atom changes not only Fe-Fe interaction, but also Fe-X interaction, and the latter is dependent on the chemical properties of X atoms. It can be concluded that, based on our results, the chemical bonding effect in $R-(Fe,M)_{12}-X$ is determined by the features of the Fe-X bonds. The role of the X atom is not only to increase the magnetic moments and hyperfine fields through magnetovolume effects, but also to affect those by chemical-bonding effects. The chemical-bonding effect is strongly dependent on the X atom. [S0163-1829(97)03147-0]

I. INTRODUCTION

It has been shown that the magnetic properties of R_2Fe_{17}(2:17) and $R(Fe,M)_{12}$(1:12) compounds (R=rare earth, M=Ti,Mo,V, etc.) can be improved by introducing interstitial atoms H, C, or N.[1–4] In the case of $R(Fe,M)_{12}$ compounds, by introducing the nitrogen atoms into crystallographic lattice, the Curie temperature (T_c) was found to be increased by 200 K on the average, and the Fe magnetic moments increase by 10−20%. In addition, the crystal environment of the rare-earth atoms is also significantly modified, resulting in a strong easy-axial anisotropy for $R(Fe,M)_{12}N_x$ when R=Nd, Pr, Tb, Dy, and Ho.[2] Due to these effects, $R(Fe,M)_{12}N_x$ has been considered as a new series of promising hard magnetic materials. Therefore, the interstitial doping effect has attracted interest not only in the physical aspect but also in the development of magnetic materials for technological applications.

To clarify the origin of the improvement of these magnetic properties, many experimental and theoretical studies have been carried out for R-Fe-X interstitial compounds, particularly for $R_2Fe_{17}(C,N)_x$ compounds. It is generally assumed that effects produced by interstitial atoms could be decomposed into two parts: the magnetovolume effect and chemical bonding effect. Theoretically, Jaswal *et al.*[5] have calculated the electronic structure of the $R_2Fe_{17}N_x$ compound. The competing effects of volume expansion and hybridization between the interstitial atoms and the neighboring Fe atoms in $Y_2Fe_{17}X$ (X=H,C,N) and $Gd_2Fe_{17}X$ (X=C,N,O,F) have been discussed by Beuerle *et al.*[6] and Uebele *et al.*,[7] respectively.

Theoretically, a lot of work has been done on 1:12 alloys as reviewed by Suski.[8] Band calculations were carried out for $YFe_{12-x}M_x$ (M=V, Cr, Ti, Mo, and W) by Coehoorn,[9] and Al-Omari *et al.*,[10] and for $YFe_{10}M_2$ (M=Cr and V) by Jaswal *et al.*[11] Trygg *et al.*[12] have carried out band calculations for $GdFe_{12}$, and Fernando *et al.*[13] have calculated the electronic structures of $NdFe_{11}Ti$, $NdCo_{10}V_2$, and $YCo_{10}Si_2$. To investigate the effects of interstitial atoms, the 1:12 system with a relative simple crystal structure will be more convenient, in comparison to the 2:17 compounds. It has been shown that there is only one interstitial site and it can absorb one interstitial atom in a unit formula. First-principles calculations regarding 1:12 nitrides have been performed by several authors. However, the former papers mainly concentrate on the local magnetic moments of these compounds. For instance, Sakuma[14] and Li *et al.*[15] have calculated the electronic structures of $YFe_{11}TiN$. Jaswal[16], Hu *et al.*[17] and Fernando *et al.*[13] have calculated the electronic structures of $NdFe_{11}TiN$. Asano *et al.*[18] and Ishida *et al.*[19] have studied those of $RFe_{12}X$ (X=C,N) and $YFe_{12-x}Mo_xN$ with a hypothetical lattice constants, respectively. The question of the chemical bonding effect in $YFe_{11}TiN$ compound is still an object of controversy in the literature. Sakuma[14] suggested that the chemical effect will further increase the total magnetic moment in the nitrides, while Li *et al.*[15] confirmed that there is a negative contribution to the total magnetic moment due to the nitrogen. No theoretical results for hydrides and carbides have been reported so far.

Furthermore the hyperfine field (HF) and isomer shift (IS) are two important parameters of the hyperfine interaction, which depend sensitively on the properties of the ground states. Recently, the Fermi-contact hyperfine fields ($H_{\rm FC}$) of $RFe_{12}X$ (X=C,N) have been calculated by Asano *et al.*[18]

In order to investigate the effects of the interstitial atoms on the electronic structures and hyperfine interaction in the R-$(Fe,M)_{12}$-X system, in this work, the crystallographic structures of the $YFe_{10}Mo_2$ and $YFe_{10}Mo_2X$ (X=N,H) are

TABLE I. Refinement parameters of $YFe_{10}Mo_2$ and $YFe_{10}Mo_2$(N,H) at room temperature. n is the occupation factor, x, y, z are the fractional position coordinates; m is the magnetic moment (μ_B). Numbers in parentheses are the statistical errors given by the refinement program.

$YFe_{10}Mo_2$	$a=b=8.572$ (Å), $c=4.809$ (Å), $R_I=3.02\%$, $R_F=2.47$, $T_C=360$ K				
	n	x	y	z	m
Y($2a$)	1.0	0	0	0	0
Fe($8i$)	0.48(1)	0.359(1)	0	0	1.3(3)
Mo($8i$)	0.52(2)	0.359(1)	0	0	0
Fe($8j$)	1.0	0.279(1)	0.50	0	1.3(3)
Fe($8f$)	1.0	0.25	0.25	0.25	1.3(3)
$YFe_{10}Mo_2N$	$a=b=8.694$ (Å), $c=4.816$ (Å), $R_I=3.80\%$, $R_F=3.03$, $T_C=450$ K				
	n	x	y	z	m
Y($2a$)	1.0	0	0	0	0
Fe($8i$)	0.48(2)	0.360(1)	0	0	1.6(3)
Mo($8i$)	0.52(2)	0.360(1)	0	0	0
Fe($8j$)	1.0	0.282(1)	0.50	0	1.6(3)
Fe($8f$)	1.0	0.25	0.25	0.25	1.6(3)
N($2b$)	0.99(2)	0	0	0.50	0
$YFe_{10}Mo_2H$	$a=b=8.592$ (Å), $c=4.817$ (Å) $R_I=3.96\%$, $R_F=3.03$, $T_C=440$ K				
	n	x	y	z	m
Y($2a$)	1.0	0	0	0	0
Fe($8i$)	0.46(1)	0.356(5)	0	0	1.4(1)
Mo($8i$)	0.54(2)	0.356(5)	0	0	0
Fe($8j$)	1.0	0.281(0)	0.50	0	1.4(1)
Fe($8f$)	1.0	0.25	0.25	0.25	1.4(1)
H($2b$)	0.83(1)	0	0	0.50	0

determined by neutron diffraction measurements. And the self-consistent spin-polarized linear-muffin-tin-orbital (LMTO) band calculations have been performed on $YFe_{10}Mo_2X$ (X=H,B,C,N,O,F) and $YFe_{10}Mo_2E$, which is $YFe_{10}Mo_2$ with an empty sphere insertion. Furthermore, the numerical results of their H_{FC} and IS are presented. In accordance with our results, the effects of the X atoms on the electronic structures, magnetic moments, H_{FC} and IS are discussed. To our knowledge, our paper represents the first systematic study of both electronic structures and hyperfine interaction on this magnetic system.

II. EXPERIMENTAL METHODS

The alloy $YFe_{10}Mo_2$ was prepared by arc melting using 99.9% pure metals. The nitrides were formed by heating fine powder samples in approximately 1 bar of nitrogen at 580 °C for 4 h. The hydrides were prepared by heating fine powder samples in approximately 1 bar of hydrogen at 250°C for 4 h. Standard x-ray diffraction with Cu $K\alpha$ radiation and thermomagnetic analysis were used for checking the quality of the samples. The $YFe_{10}Mo_2$ and $YFe_{10}Mo_2X$ (X=N,H) are single phases, except for a small amount of α-Fe in nitrides, which is inevitable in the nitrogenation process.[20] Neutron diffraction experiments were carried out on a triple-axis spectrometer at China Institute of Atomic Energy of which the analyzer is available to improve resolution and decrease inelastic background. The neutron diffraction data were analyzed by Izumi's Rietveld structure refinement program REIEAN.[21]

III. CALCULATION DETAILS

The LMTO-ASA method[22,23] has been employed to perform a semirelativistic band calculation in the frame of the local spin density (LSD) functional theory. The exchange and correlation term takes the form deduced by von Barth and Hedin,[24] with the parameters given by Janak.[25] The s, p, and d orbitals are used for Y, Fe, Mo, and s, p orbitals are used for X atoms. The atoms sphere radii are chosen to be $r_Y:r_{Fe}:r_{Mo}=1.35:1:1.12$ following Ref. 9. The atomic sphere radius for the X atom is set at $r_X/r_{Fe}=0.6$. The calculation is performed for 126 K points in the irreducible parts of the Brillouin zone. The atomic positions of $YFe_{10}Mo_2$ and $YFe_{10}Mo_2X$ (X=E,C,B,N,H,O,F) are scaled according to our experimental results listed in Table I. In order to separate the geometrical effect of doping $YFe_{10}Mo_2$ from chemical bonding effect, we have performed the following calculations.

(1) $YFe_{10}Mo_2X$ (X=H,C,B,N,O,F) with the coordinates of the experimental lattice constants of nitrogenated $YFe_{10}Mo_2N$.

(2) $YFe_{10}Mo_2$ with the true experimental values.

(3) $YFe_{10}Mo_2$ at experimental lattice constants of the nitrogenated compounds with an empty sphere (E) at $2b$ interstitial sites. This result represents the effect of the volume expansion produced by X atoms. So the difference between (1) and (3) will give the chemical bonding effect of the X atoms. The H_{FC} and IS are calculated according to the prescription given by Akai *et al.* for scalar-relativistic calculations.[26]

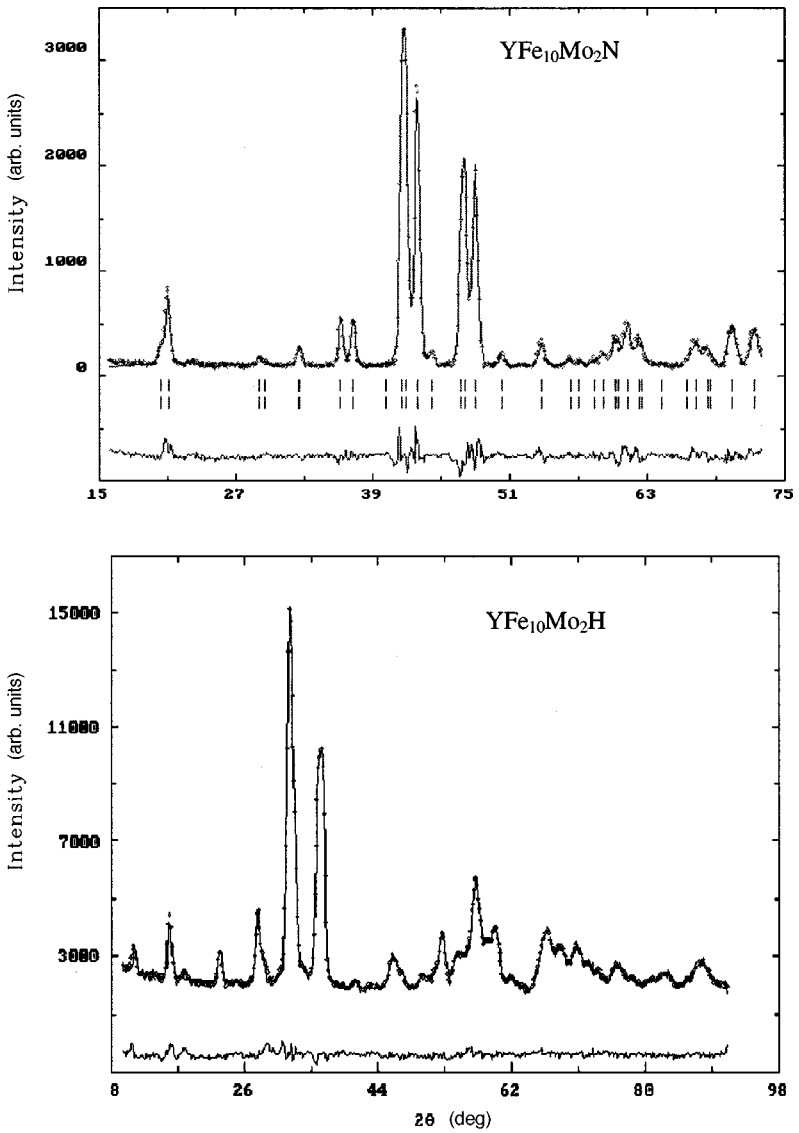

FIG. 1. The neutron diffraction patterns of $YFe_{10}Mo_2N$ and $YFe_{10}Mo_2H$.

IV. RESULTS AND DISCUSSIONS

A. Neutron diffraction data

Room-temperature neutron diffraction patterns of $YFe_{10}Mo_2H$ and $YFe_{10}Mo_2N$ are shown in Fig. 1. From Table I, the Rietveld structure analyses show that Mo atoms occupy the $8i$ sites, which is consistent with most of the experimental results.[20,27] N and H atoms are located on the $2b$ sites, which are the center of an octahedron formed by four Fe($8i$) atoms and two Y($2a$) atoms, with nearly 100% occupancy. N and H insertions result in an increase in lattice parameters with expansion mainly along the a axis. The average magnetic moments on all sites increase from 1.3 to 1.6, and 1.3 to 1.4 μ_B/atom at room temperature after nitrogenation and hydrogenation, respectively.

B. Electronic structures

Figure 2 shows the total density of states (DOS) for cases $YFe_{10}Mo_2X$ (X=E,H,B,C,N,O,F). As can be seen, the interaction between Fe($8j$) and X is strong, since there is a considerable overlap between the states of valence electrons at Fe($8j$) and those at the X site, in contrast to that between the Fe($8i$), Fe($8f$), and the X site (very weak). The higher the atomic number of the X (from H to F) is, the deeper the electronic potential of the X atom. Thus, the peaks of the DOS corresponding to the X site gradually shift to lower energy levels, and the electronic states between Fe and X are pulled down to the lower energy level. Compared with that in $YFe_{10}Mo_2E$, the energy level of $3d$ electronic at Fe($8i$), Fe($8j$), and Fe($8f$) sites are changed, and the DOS at Fermi level E_F, $N(E_F)$, is hence affected. Figure 3 represents the changes of the magnetic moments of Fe atoms μ_{Fe} at different sites with X atoms. It can be observed that the magnetovolume effect results in an increase of magnetic moments at all Fe sites, while the chemical bonding effect of X atoms increases the magnetic moments at Fe ($8f$) sites but decreases that at Fe($8j$) sites, except X=F where the chemical bonding effect is very weak. The number of spin up and spin down valence electrons at different Fe sites is given in Fig. 4. As a comparison to $YFe_{10}Mo_2E$, the insertion of the X atoms decreases the number of spin down electrons at Fe($8f$) sites but increases that at Fe($8j$) sites (except X=F), and in the meantime, the number of the spin up electrons at Fe($8f$) sites is increased. Thus a distinctively different effect on the magnetic moments μ_{Fe} at Fe($8f$) and Fe($8j$) sites was

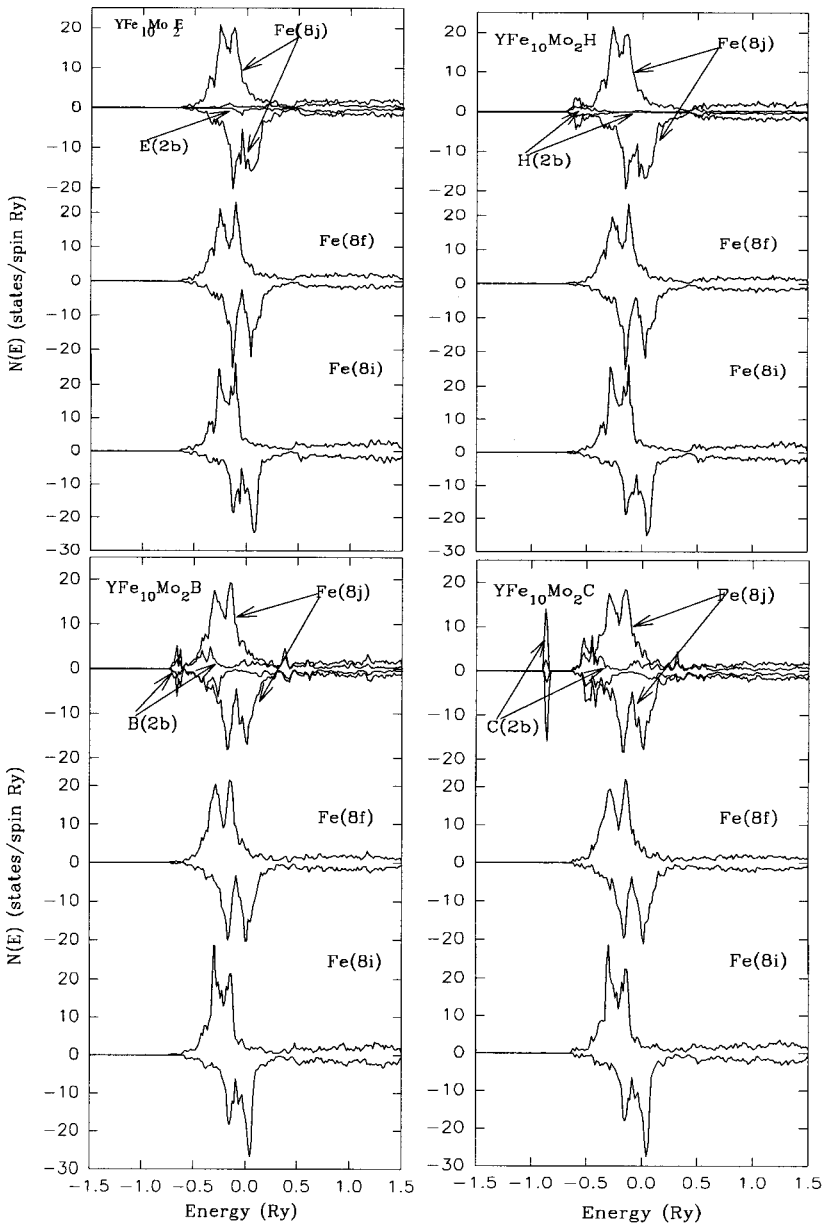

FIG. 2. Total densities of states of $YFe_{10}Mo_2E$ and $YFe_{10}Mo_2X$ (X=H,B,C,N,O,F).

found. The number of the spin up and spin down electrons at Fe($8i$) is slightly changed, then X insertion has a little effect on the magnetic moments at Fe($8i$) sites.

We can relate these results to the nearest-neighbor (NN) environment in the crystal structure, namely, the ligand number and the nearest-neighbor distances of the Fe atoms at different sites. The Fe($8j$) and Fe($8f$) have eight NN irons, while Fe($8i$) has 10.5 iron neighbor on average. The Fe-X distances are 1.93, 3.27, and 3.93 Å for $8j$, $8f$, and $8i$ sites, respectively, and and Y($2a$)-X distance is 2.40 Å. The shortest Fe($8j$)-X distance causes a strong overlap between X and Fe($8j$) states, and the iron moments at $8j$ sites are severely reduced on account of X-Fe($8j$) bond. On the other hand, the Y($2a$)-X distance is less than that of Fe($8f$)-X, and X atoms become the nearest neighbors of Y atoms. The hybridization between Y($2a$) and X atoms forms a tight covalent bond,[14,19] which would release the surrounding Fe atoms from bonding with the Y atoms. This will give rise to an increase for the magnetic moments at Fe($8f$) sites. As to Fe atoms at $8i$ sites, Fe-X distance and the Fe-Fe nearest-neighbor number are larger than those of Fe atoms at $8f$ sites. The chemical bonding effect of X atoms will have little effect on $8i$ sites due to the fact that Fe-Fe interaction are dominant at these sites.

Summarizing the influence of the X atoms on the electronic structures at Fe sites, we find that the chemical bonding effect of the X atoms is different, and changes irregularly with the increase of the atomic number of X. The iron magnetic moments of the Fe($8j$) sites are reduced by hybridization with $2s$ and $2p$ electrons of the X atoms (expect X=F). The effect is greatest for X=B, and decreases toward the end of the series. It was demonstrated that for X=B, the p states of the B atoms occur energetically in the lower part of the Fe $3d$ states, which gives rise to a strong hybridization effect, and a decrease of the magnetic moments. When going from X=B to X=C,N,O,F, the potential of the doping atom becomes steeper and steeper, the p states and s states occur at successively lower energies, and thus the hybridization effect becomes weaker and weaker. As going from C to N, O, and F, it successively arrives at a situation that is similar to the

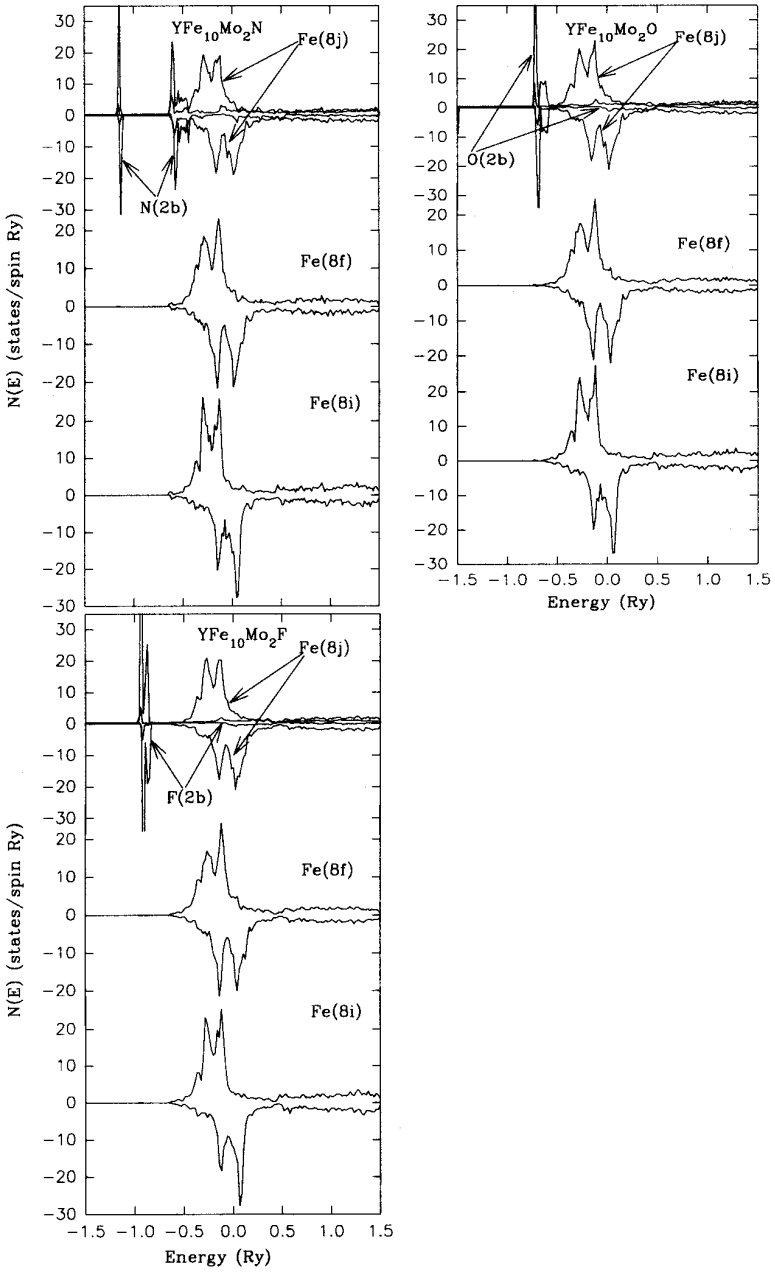

FIG. 2. (*Continued*).

case of $YFe_{10}Mo_2E$. As a result, for $YFe_{10}Mo_2F$, there is nearly no chemical bonding effect and hence just an increase of the magnetic moments due to the magnetovolume effect. It is therefore suggested that F is probably the optimum doping atom to achieve large magnetic moments in the 1:12 compounds, provided that the sample can be prepared and remain stable.

C. Hyperfine interactions

Figure 5 shows the H_{FC} at three inequivalent Fe sites in $YFe_{10}Mo_2X$ ($X=E$,H,C,B,N,O,F) as well as $YFe_{10}Mo_2$. It is easy to see that the magnetovolume effect will increase the hyperfine fields at all Fe sites and the average hyperfine fields as well. Compared with that in $YFe_{10}Mo_2E$, the chemical bonding effect of the X atoms reduced the average H_{FC} at Fe sites. The reduction in the $YFe_{10}Mo_2B$ is the largest. Considering the H_{FC} at the Fe($8i$), Fe($8j$), and Fe($8f$) sites, respectively, we find that the chemical bonding effect of the

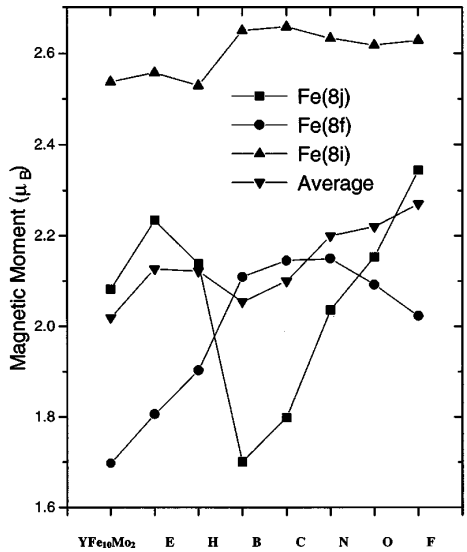

FIG. 3. The calculated magnetic moments at Fe sites in $YFe_{10}Mo_2$ and $YFe_{10}Mo_2X$ ($X=E$,H,B,C,N,O,F).

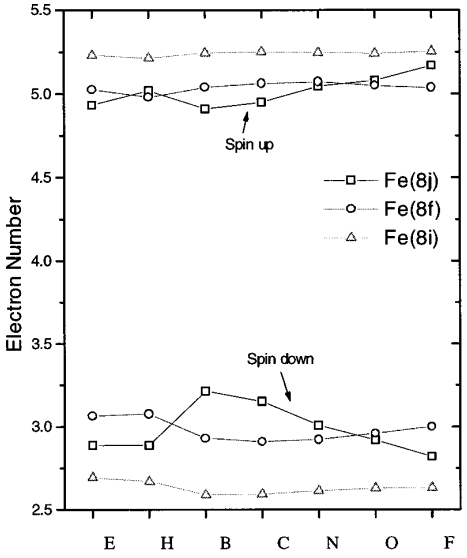

FIG. 4. The number of spin up and spin down electrons at different Fe sites in $YFe_{10}Mo_2E$ and $YFe_{10}Mo_2X$ (X=H,B,C,N,O,F).

X atoms reduces the H_{FC} at Fe($8i$) and Fe($8j$) sites, but increases that at Fe($8f$) sites. In order to compare the chemical bonding effects of different X atoms on H_{FC}, we decompose H_{FC} into two parts, H_{FC}^{core}, which is the contribution of core electrons and comes from the polarization of core due to the polarized d electrons, and H_{FC}^{val}, which comes from the polarization of valence electrons. The H_{FC}^{core} and H_{FC}^{val} contributions of H_{FC} are also shown in Fig. 5. It can be seen that H_{FC}^{core} at Fe sites is the dominant contribution to the H_{FC}. The

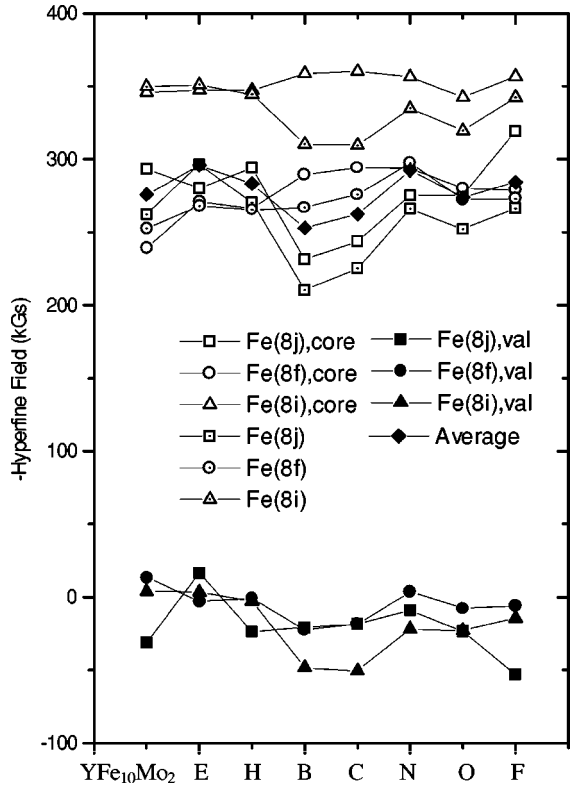

FIG. 5. The calculated hyperfine fields at different Fe sites in $YFe_{10}Mo_2$ and $YFe_{10}Mo_2X$ (X=E,H,B,C,N,O,F).

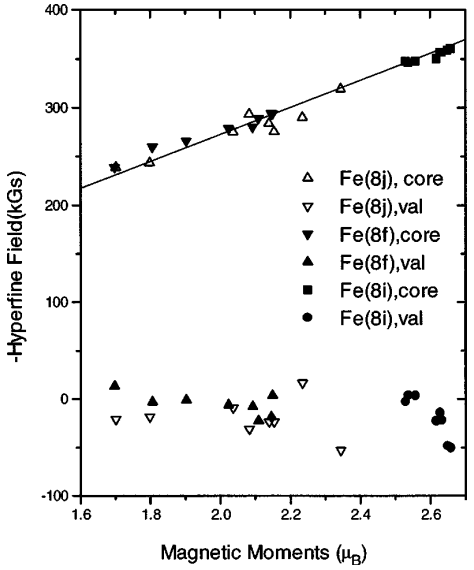

FIG. 6. The dependence of H_{FC}^{core} and H_{FC}^{val} at Fe sites on Fe magnetic moments (μ_{Fe}) in $YFe_{10}Mo_2$ and $YFe_{10}Mo_2X$ (X=E,H,B,C,N,O,F).

magnetic moment (μ_{loc}) dependence of the H_{FC}, H_{FC}^{core}, and H_{FC}^{val} at different Fe sites is shown in Fig. 6. Obviously, a linear relationship between the H_{FC}^{core} and local magnetic moments is observed, and the proportional coefficient is estimated to be about $-11T/\mu_B$, whereas the valence contribution and total hyperfine fields are not proportional to the magnetic moments, in contrast to the basic assumption that is generally made for the determination of local magnetic moments from Mössbauer experiments. Hence, it can be seen that H_{FC} at Fe sites is affected by two factors, μ_{loc} and the polarization of the valence electrons.

The H_{FC} at X sites is listed in Table II. It can be seen that the main source of H_{FC} at X sites is H_{FC}^{val} in which $H_{FC}^{t,val}$ transferred from the neighboring atoms dominates (except X=B). The difference in H_{FC} at X sites reveals that the Fe-X

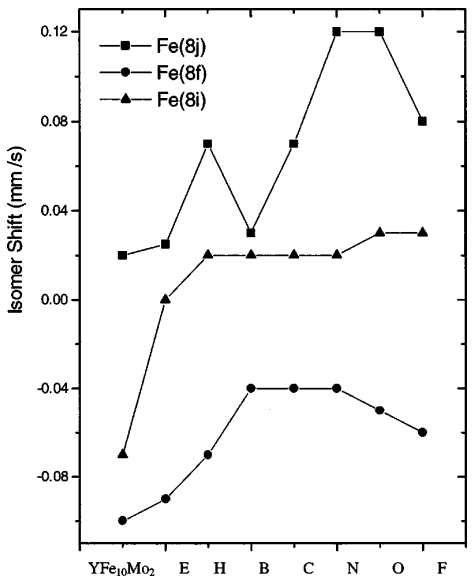

FIG. 7. The calculated isomer shifts at different Fe sites in $YFe_{10}Mo_2$ and $YFe_{10}Mo_2X$ (X=E,H,B,C,N,O,F).

TABLE II. Hyperfine fields of X atoms in $YFe_{10}Mo_2X$ (X=H,B,C,N,O,F).

$YFe_{10}Mo_2X$	H	B	C	N	O	F
H_{FC}	−5.79	1.89	31.99	43.77	146.44	129.09
H_{FC}^{val}	−5.98	−5.73	31.39	57.82	162.64	149.72
H_{FC}^{core}	0.19	7.62	0.60	−14.05	−16.20	−20.63

interaction varies strongly with the X atoms. Generally, a positive contribution to the H_{FC}^{val} at X sites is induced by antibonding states and a negative one by bonding states, where both are produced by the s-d hybridization. Our results indicate that bonding states are favored in Fe-H, Fe-B bonds while the antibonding states dominate in Fe-C, Fe-N, Fe-O and Fe-F bonds.

Figure 7 gives the calculated results of the isomer shifts at different Fe sites. The value of IS is given relative to α-Fe with a calibration constant $\alpha=-0.24a_0^3(\text{mm sec}^{-1})$.[26] As can be seen from this figure, the chemical bonding effect of the X atoms increases the IS at all Fe sites. The increase of the isomer shifts is induced by the chemical bonding effect of the X atoms which promotes the mobility of the electron and then in turn decreases the s valence charge density at nucleus sites, so the IS at Fe sites is increased. A small increase of IS at Fe($8j$) sites occurs for X=B due to a strongly s-d hybridization between B atoms, and Fe($8j$) atoms, which increases the s-d admixture.

V. CONCLUSIONS

The neutron diffraction measurements have been applied to analyze the crystallographic structure and magnetic moments of $YFe_{10}Mo_2$ and $YFe_{10}Mo_2X$ (X=H,N) and a systematic study of the magnetic moments and hyperfine interaction of the $YFe_{10}Mo_2X$ (X=H,C,B,N,O,F) and $YFe_{10}Mo_2E$ were performed by means of local-spin-density approximation and linear-muffin-tin orbital theory in atomic-sphere approximation. The nitrogen and hydrogen atoms located on the 2b interstitial sites, which have a great effect on the magnetic properties of the 1:12 compounds. The magnetovolume effect will increase the magnetic moments and hyperfine fields at all Fe sites. The chemical bonding of the X atoms changes the Fe-Fe interaction, resulting in drastic changes of the electronic structures and hyperfine parameters at Fe sites. The Fe-X interaction strongly depends on the X atoms, among all situations the B and F atoms are the most remarkable. Accordingly, the interstitial chemical bonding effect in $YFe_{10}Mo_2X$ is dominated by the characteristic of the Fe-X bonds.

ACKNOWLEDGMENTS

This work was supported by the National Natural Science Foundation and the National Target Basic Research Project. The author thanks Dr. Yong Kong and Jianzhong Zhang for their helpful discussion.

[1] J. M. D. Coey and H. Sun, J. Magn. Magn. Mater. **87**, L251 (1990).
[2] Y. C. Yang, X. D. Zhang, L. S. Kong, Q. Pan, and S. L. Ge, Appl. Phys. Lett. **58**, 2042 (1991).
[3] Z. X. Tang, E. W. Singleton, and G. C. Hadjipanayis, IEEE Trans. Magn. , **28**, 2572 (1992).
[4] S. Obbade, S. Miraglia, D. Fruchart, M. Pre, P. L'Heritier, and H. Barlet, C. R. Acad. Sci., Ser. II: Mec. Phys., Chim., Sci. Terre Univers. **307**, 889 (1988).
[5] S. S. Jaswal, W. B. Yelon, and G. C. Hadjipanayis, Y. Z. Wang, and D. J. Sellmyer, Phys. Rev. Lett. **67**, 644 (1991).
[6] T. Beuerle and I. Fähnle, Phys. Status Solidi B **174**, 257 (1992).
[7] Uebele, K. Hummler, and M. Fähnle, Phys. Rev. B **53**, 3296 (1996).
[8] W. Suski, in *Handbook on the Physics and Chemistry of Rare Earths*, edited by K. A. Gschneidner and L. Eyring (Elsevier Science B. V, Amsterdam, 1996), Vol. 22, p. 143, and references therein.
[9] R. Coehoorn, Phys. Rev. B **41**, 11 790 (1990).
[10] I. A. Al-Omari, S. S. Jaswal, A. S. Fernando, and D. J. Sellmyer, and H. H. Hamdeh, Phys. Rev. B **50**, 12 665 (1994).
[11] S. S. Jaswal, Y. G. Ren, and D. J. Sellmyer, J. Appl. Phys. **67**, 4564 (1990).
[12] J. Trygg, B. Johansson, and M. S. S. Brooks, J. Magn. Magn. Mater. **104-107**, 1447 (1992).
[13] A. S. Fernando, J. P. Woods, S. S. Jaswal, B. M. Patterson, D. Welipitiya, A. S. Nozareth, and D. J. Sellmyer, J. Appl. Phys. **73**, 6919 (1993).
[14] A. Sakuma, J. Phys. Soc. Jpn. **61**, 4119 (1992).
[15] Y. P. Li and J. M. D. Coey, Solid State Commun. **81**, 447 (1992).
[16] S. S. Jaswal, Phys. Rev. B **48**, 6156 (1993).
[17] W. Y. Hu, J. Z. Zhang, Q. Q. Zheng, and C. Y. Pan, J. Appl. Phys. **76**, 6751 (1994).
[18] S. Asano, S. Ishida, and S. Fujii, Physica B **190**, 155 (1993).
[19] S. Ishida, S. Asano, and S. Fujii, Physica B **193**, 66 (1994).
[20] H. Sun, Y. Morii, H. Fujii, M. Akayama, and S. Funahashi, Phys. Rev. B **48**, 13 333 (1993).
[21] F. Izumi, in *The Rietveld Method*, edited by R. A. Yong (Oxford University Press, Oxford, 1993), Chap. 13.
[22] O. K. Anderson, Phys. Rev. B **12**, 3060 (1975).
[23] H. L. Skliver, *The LMTO Method*, edited by M. Cardona, P. Fulde, and H. J. Queisser (Springer, Berlin, 1984).
[24] U. von Barth and L. Hedin, J. Phys. C **5**, 1629 (1972).
[25] J. F. Janak, Solid State Commun. **25**, 53 (1978).
[26] H. Akai, M. Akai, S. Blügel, B. Drittler, E. Ebert, K. Terakura, R. Zeller, and P. H. Dederichs, Prog. Theor. Phys. Suppl. **101**, 11 (1990).
[27] W. B. Yelon and G. C. Hadjipanayis, IEEE Trans. Magn. **28**, 2316 (1992).